A Shear-Flow Stabilized Z-Pinch Equilibrium

Matt Russell[1]
Independent Researcher, Richmond, VA, USA[a)]

By exchanging the non-relativistic Bennett profile from density to flow velocity, a shear-flow stabilized Z-pinch may be constructed that requires an enhanced thermodynamic gradient. The equilibrium is analytic and yields a tractable magnetic field and plasma pressure that are described by rational polynomial logarithmic forms. The equilibrium can be solved to yield accurate solutions for the current density of the DIII-D and MAST edge pedestals, an air plasma streamer head, and the axial velocities of shear-flow stabilized Z-pinch experiments from 2001 and 2009. The thermal confinement time of experimental shear-flow stabilized Z-pinches is computed accurately with this equilibrium using experimental values.

The problem of determining the analytic form of a shear-flow stabilized Z-pinch[1–3] is somewhat of a Gordian Knot. This is because the ideal Shumlak-Hartman criterion reads,

$$\frac{\mathrm{d}u_z}{\mathrm{d}r} > 0.1kV_A \tag{1}$$

where,

$$k = \frac{2\pi}{L} \tag{2}$$

$$V_A = \frac{B}{\sqrt{\rho\mu_0}} \tag{3}$$

Complicating matters further the stability of the $m = 0$ mode depends on the logarithmic gradient of the logarithmic pressure, and in the non-ideal sense shear-flow stabilization requires,

$$\frac{\mathrm{d}u_z}{\mathrm{d}r} \geq \frac{L}{2\pi r_p}\left|\frac{\mathrm{d}\ln(p)}{\mathrm{d}\ln(r)}\right| \tag{4}$$

In a plasma with arbitrary species, s, the center-of-mass momentum density giving the stabilizing shear is,

$$\vec{u} = \frac{\sum_s m_s n_s \vec{u}_s}{\sum_s m_s n_s} \tag{5}$$

and the plasma current density is,

$$\vec{J} = \sum_s q_s n_s \vec{u}_s = en\sum_s Z_s \vec{u}_s = en\vec{U} \tag{6}$$

A singly-ionized quasineutral hydrogen-electron plasma illustrates the nature of the problem at even just the ideal level, because there is simply no general way to relate the stabilizing shear to the plasma drift supporting the current density, and providing the magnetic field for a stationary system.

Instead, an attempt to solve the problem via brute-force over an ambiguous search space representing all the possible forms for the axial flows of all the possible plasma species would be necessitated, but like searching for a needle in a haystack of infinitely many of them. The futility of this search is only further evidenced by the further need there would be to evaluate logarithmic pressure gradients if a stabilizing shear profile was obtained in order to determine if the stabilization held in a non-ideal context.

There is another problem lurking in the search for a shear-flow stabilized Z-pinch. Beyond Maxwell's equations in a vacuum,

$$\nabla\cdot\vec{E} = \frac{\rho_c}{\varepsilon_0} \tag{7}$$

$$\nabla\times\vec{E} = -\frac{\partial\vec{B}}{\partial t} \tag{8}$$

$$\nabla\times\vec{B} = \mu_0\vec{J} + \frac{1}{c^2}\frac{\partial\vec{E}}{\partial t} \tag{9}$$

$$\nabla\cdot\vec{B} = 0 \tag{10}$$

there is also the need to study appropriate equations for the evolution of mass, momentum, energy and heat flux in the plasma environment carrying the shear-flow stabilized Z-pinch. Shear-flow stabilized Z-pinches are entangled with dissipative effects[4], and their non-ideal nature means that invoking a closure such as the ideal gas law, $p = nk_BT$, is incorrect to describe their plasma pressure.

The best way forward then seems to be to take the Bennett profile[5,6] in its non-relativistic form,

$$n(r) = \frac{n_0}{(1+\xi^2 r^2)^2} \tag{11}$$

$$\xi^2 = \frac{C_B n_0}{T} \tag{12}$$

$$C_B = \frac{\mu_0 e^2 u_{z,0}^2}{16k_B} \tag{13}$$

and exchange it with the uniform flow of the Bennett pinch so that we have,

$$U_z(r) = U_{z,0}\frac{T(r)^2}{(T(r)+C_B n_0 r^2)^2} \tag{14}$$

Then, let us treat this as the shear-stabilizing flow. Furthermore, we will first treat the system from the perspective of an infinitely long plasma cylinder, meaning, $R_m = \mu_0\sigma uL \to \infty$ so that the system is taken to be ideal. In order to treat the stabilizing flow as the flow supporting the plasma current density we must have a direct relationship between the two, such as,

$$\vec{U} = \vec{u} \tag{15}$$

a)Email for correspondence: russellmatt66@gmail.com

In the singly-ionized hydrogen-electron plasma this requires,

$$\vec{u}_i - \vec{u}_e = \frac{m_i}{m_i + m_e}\vec{u}_i + \frac{m_e}{m_i + m_e}\vec{u}_e \tag{16}$$

In the purely non-relativistic case we have $m_i >> m_e$ leaving us with,

$$\vec{U} = \vec{u}_i - \vec{u}_e \simeq \vec{u}_i \tag{17}$$

if the electrons are taken to be stationary. The stationarity of the electrons from the ion perspective is justified in an average sense as the large electron plasma frequency will cause the average position of the electrons to appear fixed from the slower ion timescale.

IDEAL SHEAR-FLOW STABILIZED EQUILIBRIUM

The Shumlak-Hartman criterion, Equation (1) is an ideal measure so we will treat the Reynolds magnetic number as being infinite, via means of an infinitely long plasma cylinder, $L \to \infty$. The Shumlak-Hartman criterion can then be treated as collapsing to,

$$u_z' > 0 \tag{18}$$

so long as the magnetic field we obtain from this procedure does not run to infinity. What does it take for a shear based on the flow given by Equation (14) to be shear-flow stabilized? We will consider a power-law temperature,

$$T(r) = C_T^{(n)} r^n = \frac{T_p}{r_p^n} r^n \tag{19}$$

and in accord with the behavior implied by the limit of infinite Reynolds magnetic number we will treat the system for the present moment as being ideal in order to study the consequences of this decision,

$$\frac{\partial \rho}{\partial t} + \nabla \cdot (\rho \vec{u}) = 0 \tag{20}$$

$$\frac{\partial (\rho \vec{u})}{\partial t} + (\vec{u} \cdot \nabla)\rho \vec{u} = \vec{J} \times \vec{B} - \nabla p \tag{21}$$

being the conservation of mass, and momentum absent any external sources. The energy density of an ideal magnetohydrodynamic fluid is,

$$e = \frac{p}{\gamma - 1} + \frac{1}{2}\rho u^2 + \frac{B^2}{2\mu_0} \tag{22}$$

and the conservation of energy can be expressed as,

$$\frac{\partial e}{\partial t} + \nabla \cdot \left[\left(\frac{1}{2}\rho u^2 + \frac{\gamma p}{\gamma - 1} \right)\vec{u} + \frac{B^2}{2\mu_0}\vec{u} - \frac{(\vec{u} \cdot \vec{B})}{\mu_0}\vec{B} \right] = 0 \tag{23}$$

This model assumes an isotropic pressure described by an equation of state,

$$\frac{\mathrm{d}}{\mathrm{d}t}\frac{p}{\rho^\gamma} = 0 \tag{24}$$

and neglects dissipative momentum, energy and heat flux transport from the viscous anisotropic stress tensor. For a pure shear-flow stabilized Z-pinch this is represented by,

$$P_\Pi = \overleftrightarrow{\Pi} : \nabla \vec{u} = \Pi_{zr} \frac{\partial u_z}{\partial r} \tag{25}$$

Additionally, the axisymmetric temperature can be naturally associated with a heat flux under an isotropic Fick's Law closure,

$$\vec{q} = -\kappa \nabla T \tag{26}$$

The stationary, uniform density, axisymmetric Z-pinch satisfies these equations if the momentum balance, Equation (21) integrates. The mass continuity, Equation (20) is trivialized, and so is the conservation of energy, Equation (23). The latter holds because the COM flow, and magnetic field are orthogonal, the energy density is steady, and the flow is incompressible, and axisymmetric so the divergence of energy density vanishes. Therefore, this equilibrium satisfies the equations of Ideal MHD if the plasma pressure integrates.

For the uniform density, stationary, Z-pinch the convective acceleration becomes,

$$\rho \left(\vec{u} \cdot \nabla \right) \vec{u} = \rho u_z \frac{\partial u_z}{\partial z} \hat{e}_z = 0 \tag{27}$$

Returning to Equation (18) we have for the shear of Equation (14),

$$\frac{\mathrm{d}u_z}{\mathrm{d}r} = u_{z,0} \left[\frac{2TT' C_B n_0 r^2 - 4T^2 C_B n_0 r}{(T + C_B n_0 r^2)^3} \right] \tag{28}$$

$$= 2T C_B n_0 u_{z,0} r \left[\frac{T'r - 2T}{(T + C_B n_0 r^2)^3} \right] \tag{29}$$

In the context of Equation (18) we can ignore the denominator so long as it does not equal zero. For a power law temperature this only occurs at $r = 0$ so we must concentrate our study away from this point to avoid studying an indeterminate limit. That occurs without loss of generality because we are free to specify the state of the system at the boundary for any specific problem. For the current problem $r = 0$ yields an indeterminate value for the shear at the origin. Investigating this is outside the scope of our primary objective, being to determine what is needed for this profile to be shear-flow stabilized.

Supported by the prior reasoning to look away from $r = 0$, the answer to this question then rests on the shoulders of the equation,

$$T'r - 2T > 0 \tag{30}$$

as the prefix can be discarded in the same manner as the denominator. Evaluating it leaves,

$$n > 2 \tag{31}$$

From Equation (14) it is apparent that inserting $n = 2$ will result in the collapse of the shear as the profile will become

uniform. For $n = 3$ we obtain,

$$u_z(r) = u_{z,0}\frac{r^2}{(r+C)^2} \tag{32}$$

$$C = \frac{C_B n_0}{C_T^{(3)}} = \frac{\mu_0 e^2}{16 k_B}\frac{n_0 u_{z,0}^2 r_p^3}{T_p} \simeq 10^{-22}\frac{n_0 u_{z,0}^2 r_p^3}{T_p} \tag{33}$$

where C is related to the location of maximum shear,

$$r_{max} = \frac{C}{2} \tag{34}$$

Treating Equation (32) as the drift flow supporting the plasma current density, e.g., in the regime of non-relativistic ions and stationary electrons, we have,

$$\vec{J} = J_z(r)\hat{z} = e n_0 u_{z,0}\frac{r^2}{(r+C)^2}\hat{z} \tag{35}$$

The pure axisymmetric equilibrium that we are considering obtains the magnetic field from Ampere's Law,

$$B_\theta(r) = \frac{\mu_0}{r}\int_0^r r' J_z(r') dr' \tag{36}$$

and the plasma pressure from the ideal momentum balance,

$$\nabla p = \vec{J}\times\vec{B} \tag{37}$$

which holds here because a uniform density, steady, pure Z-pinch feels no inertial forces, and gives the force balance,

$$\frac{\mathrm{d}p}{\mathrm{d}r} = -J_z B_\theta \tag{38}$$

which produces the plasma pressure,

$$p(r) = p_0 - \int_0^r J_z(r')\frac{\mu_0}{r'}\int_0^{r'} r'' J_z(r'') dr'' dr' \tag{39}$$

$$p_0 = \int_0^{r_p} J_z B_\theta dr \tag{40}$$

For the $n = 3$ case these integrals are tractable, and can be evaluated with u-substitution or via Computer Algebra System (CAS). Furthermore, the ideal equations for mass, and energy conservation are also satisfied trivially by this equilibrium given that it remains a stationary and axisymmetric pure Z-pinch.

The equilibrium magnetic field is given by,

$$B_\theta(r;\, C) = e n_0 u_{z,0}\mu_0\frac{f(r;\, C)}{2r(r+C)}\hat{\theta} \tag{41}$$

$$f(r;\, C) = f_1(r) + f_2 + f_3 + f_4 \tag{42}$$

$$f_1(r) = r^3 \tag{43}$$

$$f_2(r;\, C) = -3Cr^2 \tag{44}$$

$$f_3(r;\, C) = -6C^2 r\left(1 + \ln\left(\frac{C}{r+C}\right)\right) \tag{45}$$

$$f_4(r;\, C) = -6C^3 \ln\left(\frac{C}{r+C}\right) \tag{46}$$

IDEAL SHEAR-FLOW STABILIZATION

We will evaluate two limits of the normalized shear measure,

$$S^{(I)} = \frac{u_z'}{kV_A} = u_z'\frac{L}{2\pi}\frac{\sqrt{\rho\mu_0}}{B_\theta} \tag{47}$$

that Shumlak and Hartman originally considered. The limit of arbitrarily small plasma radius,

$$\lim_{r\to 0^+} S^{(I)} > 0.1 \tag{48}$$

and the limit of arbitrarily small pinch radius,

$$\lim_{r_p\to 0^+} S^{(I)} > 0.1 \tag{49}$$

Evaluating Equation (48) and Equation (49) here depends on evaluating the limits of the function,

$$S(r) = \frac{u_z'}{B_\theta} = \frac{4C}{e n_0\mu_0}\frac{r^2}{(r+C)^2}\frac{1}{f(r,C)} \tag{50}$$

For the limit as plasma radius goes to zero $S(r)$ is indeterminate. Two applications of L'Hopital's rule are required to lift it yielding,

$$\lim_{r\to 0^+} S(r) = \frac{4C}{e n_0\mu_0}\lim_{r\to 0^+}\frac{2}{(r+C)^2 f'' + 4(r+C)f' + 2f} \tag{51}$$

which diverges because $f(0^+,C) = f'(0^+,C) = f''(0^+,C) = 0$ while the numerator remains finite and non-zero. So, this equilibrium is shear-flow stabilized in an ideal sense for arbitrarily small plasma radius.

For arbitrarily small pinch radius we have,

$$C = \tilde{C} r_p^3 \tag{52}$$

so that,

$$\lim_{r_p\to 0^+} S(r) = \frac{4}{e n_0\mu_0}\tilde{C} r_p^3\frac{r^2}{(r+\tilde{C}r_p^3)^2}\frac{1}{f(r,\tilde{C}r_p^3)} \tag{53}$$

We consider a scaling relationship between r, and r_p,

$$r = \alpha r_p \tag{54}$$

so that we have,

$$\lim_{r_p\to 0^+} S(r) = \frac{4}{e n_0\mu_0}\tilde{C}\alpha^2\lim_{r_p\to 0^+}\frac{r_p^3}{(\tilde{C}r_p^2+\alpha)^2}\frac{1}{f(\alpha r_p,\tilde{C}r_p^3)} \tag{55}$$

$$= \frac{4}{e n_0\mu_0}\tilde{C}\alpha^2\lim_{r_p\to 0^+}\frac{r_p^3}{\alpha^2}\frac{1}{r^3} \tag{56}$$

$$= \frac{4}{e n_0\mu_0}\frac{\tilde{C}}{\alpha^3} \tag{57}$$

Plugging this back into Equation (49) we arrive at the limiting condition,

$$20L\frac{\sqrt{\rho\mu_0}}{\pi e n_0\mu_0}\frac{\tilde{C}}{\alpha^3} > 1 \tag{58}$$

which is strongly satisfied towards the axis.

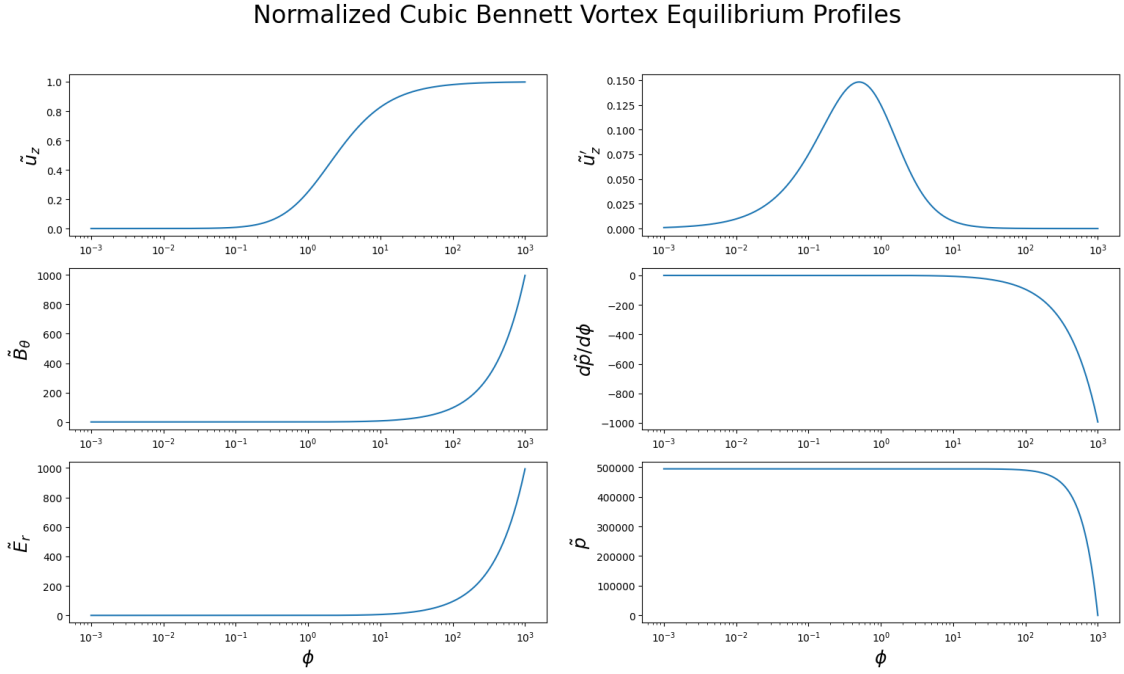


FIG. 1. Normalized profiles for the equilibrium properties, $\tilde{u}_z$, $\tilde{u}'_z$, $\tilde{B}_\theta$, $\frac{d\tilde{p}}{d\tilde{\phi}}$, $\tilde{E}_r$, and $\tilde{p}$ of the pure-flow vortex. The density is not plotted because it is uniform. The profiles are normalized not by the maximum value, but by a physical normalization derived from the non-dimensionalization process.

NON-IDEAL SHEAR-FLOW STABILIZATION

We will evaluate two limits of the normalized shear measure based on the non-ideal AWDG shear criterion,

$$S^{(NI)} = \frac{u'_z r_p}{\left|\frac{\mathrm{d}\ln(p)}{\mathrm{d}\ln(r)}\right|} \tag{59}$$

where the limit of arbitrarily small plasma radius becomes,

$$\lim_{r\to 0^+} S^{(NI)} > \frac{L}{2\pi} \tag{60}$$

and the limit of arbitrarily small pinch radius,

$$\lim_{r_p\to 0^+} S^{(NI)} > \frac{L}{2\pi} \tag{61}$$

The construction of the non-ideal criterion here based on Angus et. al's work is made on the approximate recommendations presented there. A non-trivial vacuum pressure is now required,

$$p_0 = p_{vac} + \int_0^{r_p} J_z B_\theta dr \tag{62}$$

because the logarithmic pressure gradient becomes,

$$\frac{\mathrm{d}\ln(p)}{\mathrm{d}\ln(r)} = -r\frac{J_z(r)B_\theta(r)}{p(r)} \tag{63}$$

so the value will diverge to infinity at the pinch radius if $p_{vac} = 0$. It is acceptable to treat the amplitude of this as,

$$\left|\frac{\mathrm{d}\ln(p)}{\mathrm{d}\ln(r)}\right| = r\frac{J_z B_\theta}{p(r)} \tag{64}$$

because both the numerator, and denominator are positive for all non-trivial plasma radius, r, and shear localization, C. With $J_z(r) = en_0u_z(r)$ then we have,

$$S^{(NI)} = \frac{2r_pC}{en_0}\frac{1}{r^2(r+C)}\frac{p(r)}{B_\theta(r)} \tag{65}$$

so that the limit in the context of an arbitrarily small plasma radius becomes,

$$\lim_{r\to 0^+} S^{(NI)} = \infty \tag{66}$$

meaning this equilibrium is shear-flow stabilized for an arbitrarily small plasma radius.

In the limit of arbitrarily small pinch radius we again fix the plasma radius at which we are observing the system as a fraction of the pinch radius so that it does not slide outside of the system bounds as we are taking the limit. Then, evaluating this we obtain,

$$x = \frac{r}{r_p} \tag{67}$$

$$\lim_{r_p\to 0^+} S^{(NI)}(xr_p, r_p) = \frac{1}{4k_BT_p}\frac{u_{z,0}}{n_0}\frac{p_{vac}}{x^4} \tag{68}$$

so that for fixed normalized radius we have a limiting condition which becomes strongly satisfied as we move towards the axis, i.e., $x \to 0^+$ which is valid in the context of the limit we took as we can always choose an r smaller than whatever r_p is as we contract the latter to maintain consistency.

APPLICATIONS

To apply this equilibrium, we must solve it. In general we can treat the boundary conditions as,

$$u(0) = u_0 \tag{69}$$
$$u(r_p) = u_{edge} \tag{70}$$

so that the flow profile can either rise up or down,

$$u_z(r) = u_0 \pm u_{z,0}\frac{r^2}{(r+C)^2} \tag{71}$$

Plasmas with current densities described by this flow profile,

$$J_z(r) = en_0\left(u_0 \pm u_{z,0}\frac{r^2}{(r+C)^2}\right) \tag{72}$$

remain shear-flow stabilized under the same conditions as when there is no core flow, because the shear remains the same, and the magnetic field picks up a linear term. The boundary conditions encode a fourth-order algebraic system whose roots give the value of the flow speeds,

$$r_p^2\left(u_{edge} - u_0 \mp u_{z,0}\right) + \tag{73}$$
$$(u_{edge} - u_0)C_u u_{z,0}^2\left(C_u u_{z,0}^2 + 2r_p\right) = 0 \tag{74}$$
$$C = C_u u_{z,0}^2 \tag{75}$$

When non-dimensionalized using the three numbers,

$$\mathrm{Ur}_{z,0} \equiv \frac{u_{z,0}}{u_0} \tag{76}$$
$$\mathrm{Ru} \equiv \frac{u_{edge}}{u_0} \tag{77}$$
$$\mathrm{Vo}^2 \equiv \frac{r_p^2}{C_u^2 u_0^4} \tag{78}$$

the system can be written simply,

$$\mathrm{Ur}_{z,0}^4 + 2\mathrm{Vo}\mathrm{Ur}_{z,0}^2 \mp \frac{\mathrm{Vo}^2}{\mathrm{Ru}-1}\mathrm{Ur}_{z,0} + \mathrm{Vo}^2 = 0 \tag{79}$$

to give a fourth-order system whose algebraic roots are the physical flow speeds of this shear-flow stabilized equilibrium. It is possible for these roots to be complex, in which case the speed, pressure, current density, and any other complex amplitudes would need to be curtailed from a complex modulus squared,

$$|u_{z,0}| = \sqrt{u_{z,0}u_{z,0}^*} \tag{80}$$

However, only real speeds correspond to physically admissible vortices as complex solutions will not in general give profiles that satisfy the boundary conditions when turned into a speed because the modulus of a root does not in general produce another root. This solution process is employed across three different domains to accurately reconstruct or produce either the axial flow velocity or plasma current density of three different systems.

There is an immediate self-similar property to this system that can be seen from considering the definition for,

$$C_u = \frac{\mu_0 e^2}{16k_B}\frac{n_0}{T_p}r_p^3 \tag{81}$$

as for fixed pinch radius, r_p, the plasma number density and edge temperature can be both varied by the same constant to give the same C_u, and therefore flow solution, while changing the plasma state in a way that maintains,

$$n_0^{(A)}T_p^{(B)} = n_0^{(B)}T_p^{(A)} \tag{82}$$

between the two self-similar shear-flow stabilized plasma equilibrium states.

Zap 2001 & 2009

The microscopic nature of this profile's shear-flow stability suggests solving for a chain of these vortices across the experimental data of the axial flow speeds obtained from the 2009 DD fusion plasma experiment by carbon-III Doppler broadening. This data constitutes multiple shots, and a representative one is shown in Figure (2).

It also bears studying what occurs when the equilibrium is solved globally on the axial profiles of the DD fusion plasma experiments. This is done for data from an earlier study where the concept was demonstrated experimentally[7]. The solutions produced are shown in Figures (3), and (4).

The thermal lifetime obtained from a 0D ideal steady state power balance for the isotropic heat flux closure is,

$$\tau_E = \frac{p_0 r_p^2}{4\kappa_\perp(r_p)T_p} \tag{83}$$

where the perpendicular ion thermal conductivity is obtained from Spitzer.

Interestingly, the accurate solutions shown there are based on complex flow roots. These cause this analytic nonlinear profile to localize the shear layer incorrectly here while providing accurate values for the peak shear $S_{\mathrm{peak}} \sim 3\times 10^6\ [\mathrm{s}^{-1}]$ when compared to experiment, $S_{\mathrm{exp}} \sim 2-4\times 10^6\ [\mathrm{s}^{-1}]$. Nonetheless, the solutions presented here evidently closely capture subtleties in the nonlinear structure of the profile, albeit only within a limited range, and while being based on complex-valued flow speed roots. All this alongside being ensconced within an ideal model that neglects dissipation, and uses the core temperature instead as the edge temperature.

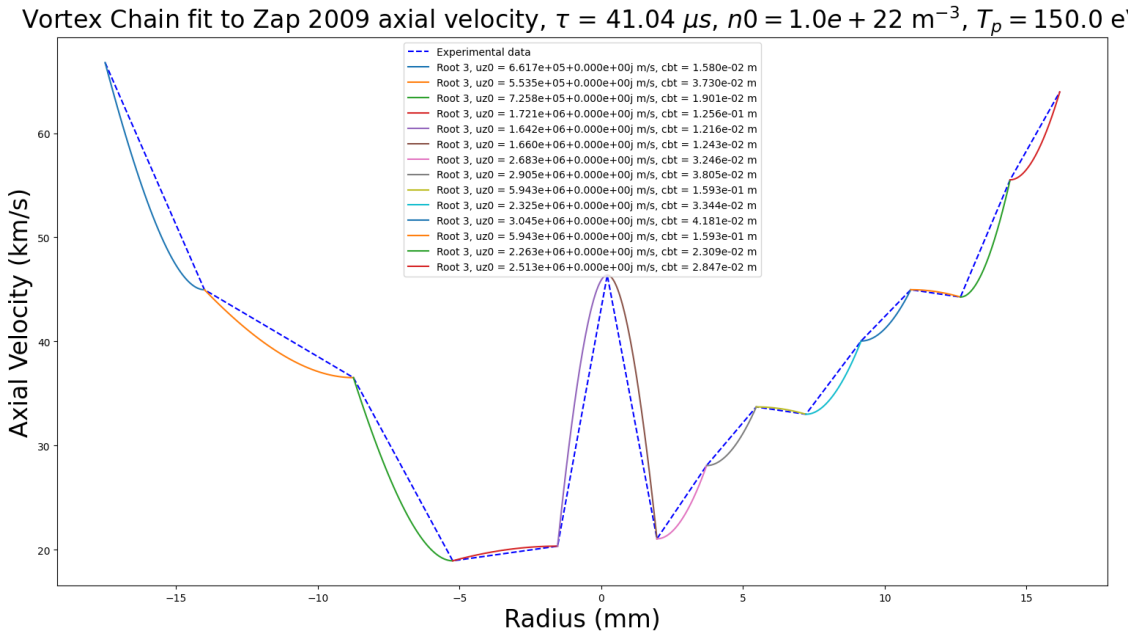


FIG. 2. Analytic reconstruction of the axial velocity profile from the 2009 Zap DD fusion plasma experiment. Each cell represents a specific solution to the vortex defined by the leftmost point being treated as the core, and the rightmost as the edge. The core temperature and number density are used as representative values here for calculating each vortex.

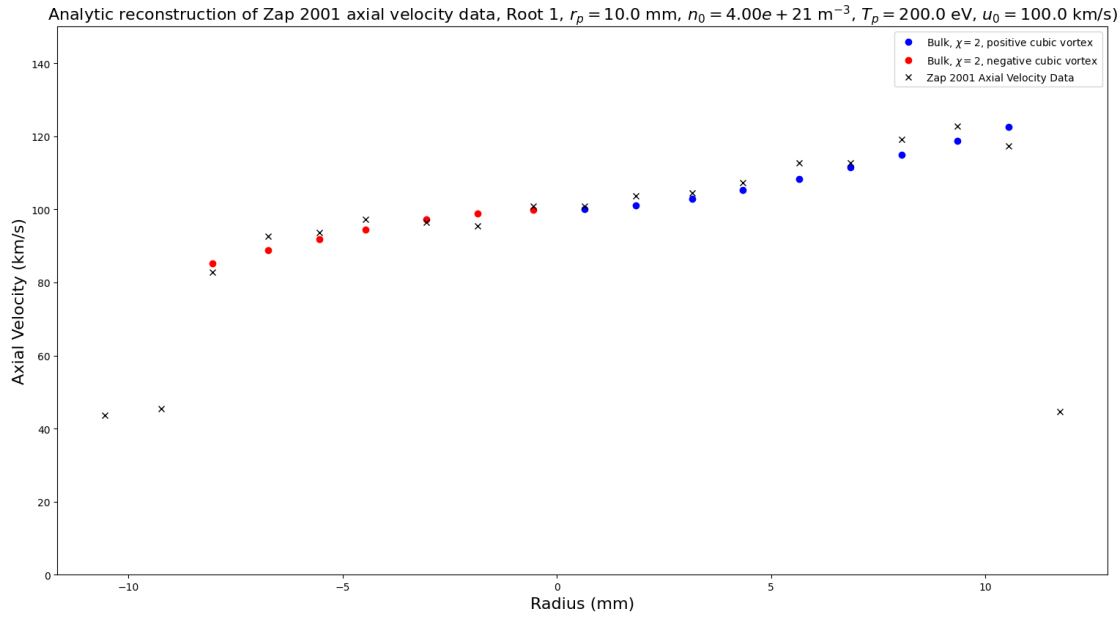


FIG. 3. Single vortex solutions to the axial velocity profile from the 2001 Zap DD fusion plasma experiment. Each pinch is calculated in the uncorrelated pinch basis, and the pinch midpoint is chosen as the connection point between the two. The flow roots for each vortex are complex-valued, $u_{z,0R} = 1.19027 \times 10^5 + j3.30410 \times 10^5$ m/s for the vortex on the right-hand side, and $u_{z,0L} = -1.19027 \times 10^5 + j3.30410 \times 10^5$ m/s for the left-hand side. The peak shear of the profiles is the same on both sides $S_{\text{peak},+} = S_{\text{peak},-} = 3.352 \times 10^6$ [s^{-1}]. The peak shear obtained from amongst all the roots is $S_{\text{peak}} = 1.4 \times 10^7$ s^{-1}. The thermal lifetime is calculated to be 13.029 μs for the negative vortex on the left, and 20.754 μs for the positive vortex on the right.

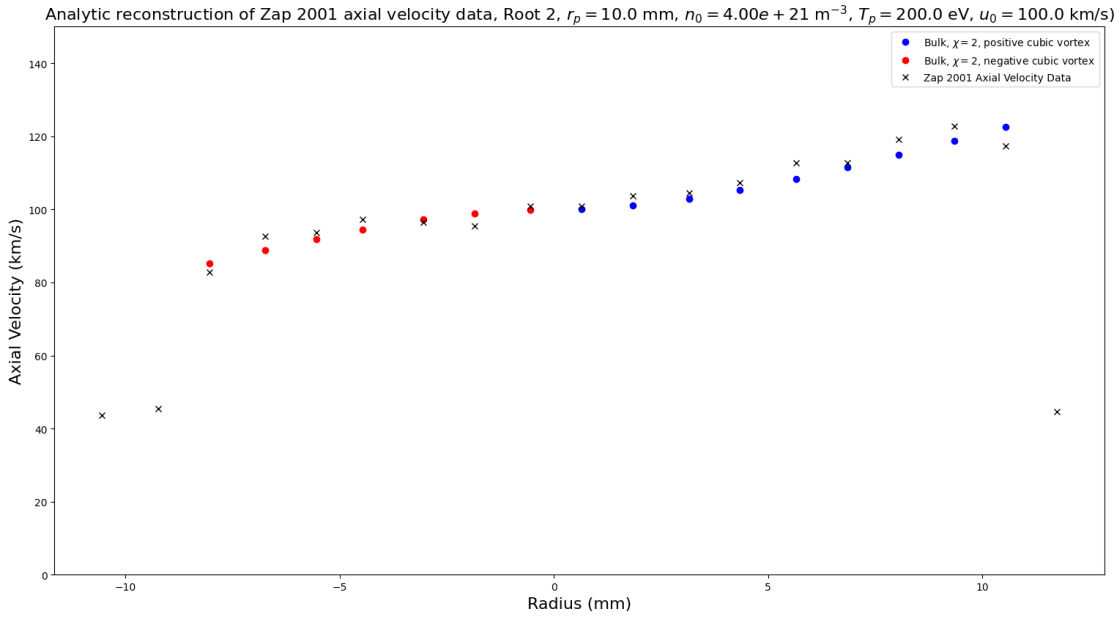


FIG. 4. Single vortex solutions to the axial velocity profile from the 2001 Zap DD fusion plasma experiment. Each pinch is calculated in the uncorrelated pinch basis, and the pinch midpoint is chosen as the connection point between the two. The flow roots for each vortex are complex-valued, $u_{z,0R} = 1.19027 \times 10^5 - j3.30410 \times 10^5$ m/s for the vortex on the right-hand side, and $u_{z,0L} = -1.19027 \times 10^5 - j3.30410 \times 10^5$ m/s for the left-hand side. The peak shear of the profiles is the same on both sides $S_{\text{peak},+} = S_{\text{peak},-} = 3.352 \times 10^6$ [s^{-1}], and the same as for the analytic solutions in Figure (3). The peak shear obtained from amongst all the roots is $S_{\text{peak}} = 1.4 \times 10^7$ s^{-1}. The thermal lifetime is calculated to be 13.029 μs for the negative vortex on the left, and 20.754 μs for the positive vortex on the right.

Air Plasma Streamer Head

A reaction-drift-diffusion study from 2021[8] of an air plasma streamer head provides an interesting study as the experimental axial light emission profile features small-scale, high-amplitude fluctuations that are suggestive of nonlinear microscale behavior. The global structure of the axial emission intensity can be linked to the plasma current density via a linear discharge model,

$$I_z = \alpha J_z \tag{84}$$

Using experimental data analytic solutions are produced, and all the roots shown in Figure (5) for one of the particular cases addressed. This axisymmetric study does not report plasma temperature or gradient, but the simulated axial electric field is suggestively zero everywhere inside the streamer volume as it would be for an ideal Z-pinch equilibrium where the force balance is supported by the radial pressure gradient and Lorentz force.

Other features of the single air plasma streamer reported in this study are suggestive of a shear-flow stabilized Z-pinch component akin to the kind studied here. For example, the uniform density along the axial chords, and steady voltage. The study in question lists twenty-nine (29) separate plasma-chemical reactions of interest while simulating 17 of them. From the context of an isotropic multi-fluid model the collisional exchange of momentum can be treated as resulting in a net zero sum between all the species. Then, each species that is in a stationary, uniform density, axisymmetric Z-pinch will be described by a balance between electric field, plasma pressure gradient, and Lorentz Force as the inertial forces disappear in such an equilibrium. This electric field comes from Gauss' Law,

$$\nabla \cdot (\varepsilon_0 \nabla \phi) = -\rho_C \tag{85}$$

and would not be stationary in time if substantial inertial forces were being felt by any plasma species as these would result in a time-dependent space charge developing where,

$$\rho_C = \sum_s e Z_s n_s \tag{86}$$

Tokamak Edge Pedestal

A parameter sweep is performed across the experimental data of the MAST edge pedestal[9], and the algebraic flow system is solved for each pair of $\{n_0, T_p\}$. The most accurate solution is collected from amongst the roots as measured by a range-normalized relative root mean square error,

$$RNRRMSE = \frac{1}{max(\hat{J}_\phi) - min(\hat{J}_\phi)} RRMSE(J, \hat{J}_\phi) \tag{87}$$

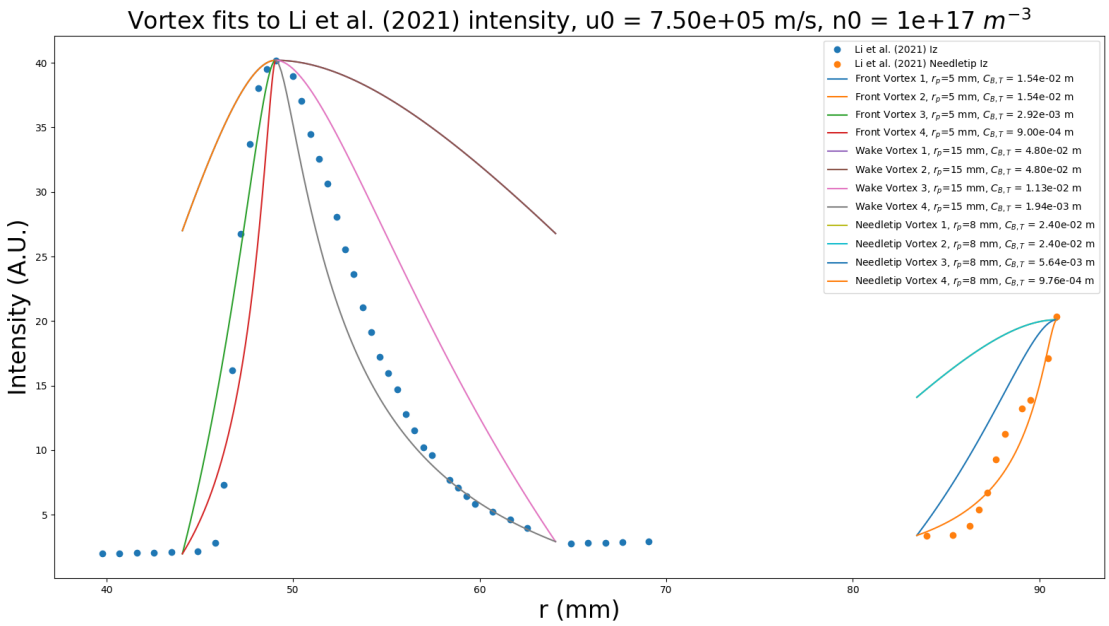


FIG. 5. Analytic vortex solution to the needletip (rightmost), front (leftmost), and wake emission intensities of an air plasma streamer head translating axially. The needletip density is $n_0 = 1 \times 10^{19}$ $[m^{-3}]$. The edge temperature of the front is $T_{p,front} = 2{,}000$ $[K]$, and the edge temperature of the wake is $T_{p,wake} = 20{,}000$ $[K]$. The values for pinch radius were chosen manually, $r_{p,\text{front}} = 5$ mm, $r_{p,\text{wake}} = 15$ mm, and $r_{p,\text{needletip}} = 7.5$ mm. The needletip density is treated as having number density $n_{0,\text{needletip}} = 10^{18}$ $[m^{-3}]$, and edge temperature, $T_{p,\text{needletip}} = 10^4$ [K]. A parameter sweep should be run over a fine neighborhood of the experimental values here in order to determine the density of accurate solutions which can be found, and a sweep over which point to use as the base. The needletip also appears to have a double vortex structure.

and every such one of these solutions which measured at less than 10% of this sort of error is shown in Figure (6). The application of a cylindrical equilibrium to a toroidal current density is acceptable here because any curvature-based corrections to this zeroth-order model can be written as a series in the parameter $\varepsilon_M = \frac{r_p}{R_C}$,

$$J_\phi = J_z + \sum_{i=1}^{n} \varepsilon_M^i J_\phi^{(i)} \tag{88}$$

So, for $r_p << R_C$, which is satisfied for $r_p \sim [mm]$, and $R_C \sim [m]$ as observed in these experiments we then have,

$$J_\phi \approx J_z \tag{89}$$

which is supported by the obtainment of the results in Figure (6) for the MAST edge pedestal. Figure (7) shows the results of the same sweep procedure performed across the DIII-D edge pedestal[10] using one of the plateau values as the connection point. Figure (8) shows another result of the sweep for a different choice of connection point.

Beyond this, the edge pedestal is a confinement barrier that appears in the presence of an enhanced thermodynamic gradient, which is also required here in order for the non-relativistic Bennett vortex to be shear-flow stabilized, and provide a confinement barrier for its thermal lifetime.

An additional property of this equilibrium is its compatibility with the existence condition for generalized Boozer coordinates[11],

$$\oint dl(\vec{J} \cdot \nabla \psi)/B = 0 \tag{90}$$

The cylindrical equilibrium considered here has $\vec{J} = J_z(r)\hat{z}$, and $\nabla\psi || \hat{e}_r$, so $\vec{J} \cdot \nabla\psi = 0$ identically. So, the zeroth-order equilibrium consequently satisfies the integral condition. Whether this property remains satisfied when finite-curvature corrections are introduced depends on the higher-order toroidal current structure.

1D Navier-Stokes

This equilibrium provides a 1D simple flow, i.e., Category 1 solution to the uniform viscosity, incompressible Navier-Stokes momentum equation on the loci $r = 3C$, and $z = 0$. For the uniform density axisymmetric Z-pinch the inertial forces disappear, and this equation reads,

$$\nu \nabla^2 \vec{u} = \frac{1}{\rho} \nabla p \tag{91}$$

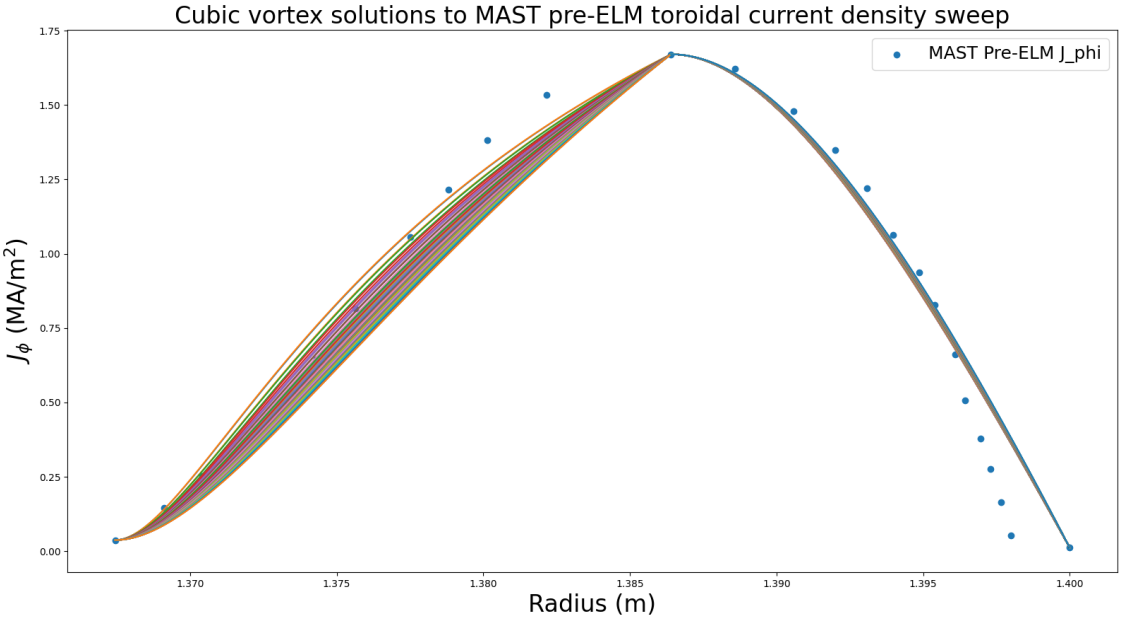


FIG. 6. Parameter sweep of the MAST edge pedestal across the span $n_0 \in [10^{19}, 10^{20}]$ m^{-3}, $T_p \in [200, 300]$ eV with $N = 25 * 25$ total value-pairs swept through. Every band represents a solution obtained from the analytic model here with less than 10% range-normalized relative root mean square error. The front region is to the right of the connection point, and the wake is to the left. The average core pressure of the wake solutions is calculated to be $< p_0 >= 2.997$ [kPa] with a standard deviation, 2.481[kPa], and median 2.362 [kPa].

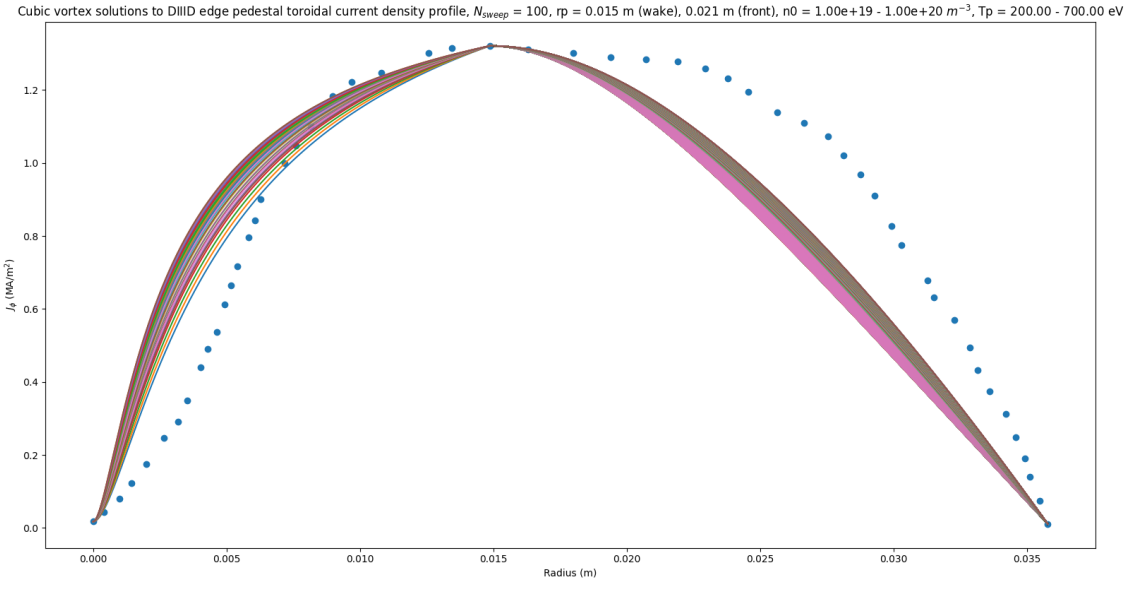


FIG. 7. Parameter sweep of the DIII-D edge pedestal across the span $n_0 \in [10^{19}, 10^{20}]$ m^{-3}, $T_p \in [200, 700]$ eV with $N = 100 * 100$ total value-pairs swept through. Every band represents a solution obtained from the analytic model here with less than 20% range-normalized relative root mean square error. The front region is to the right of the connection point, and the wake is to the left.

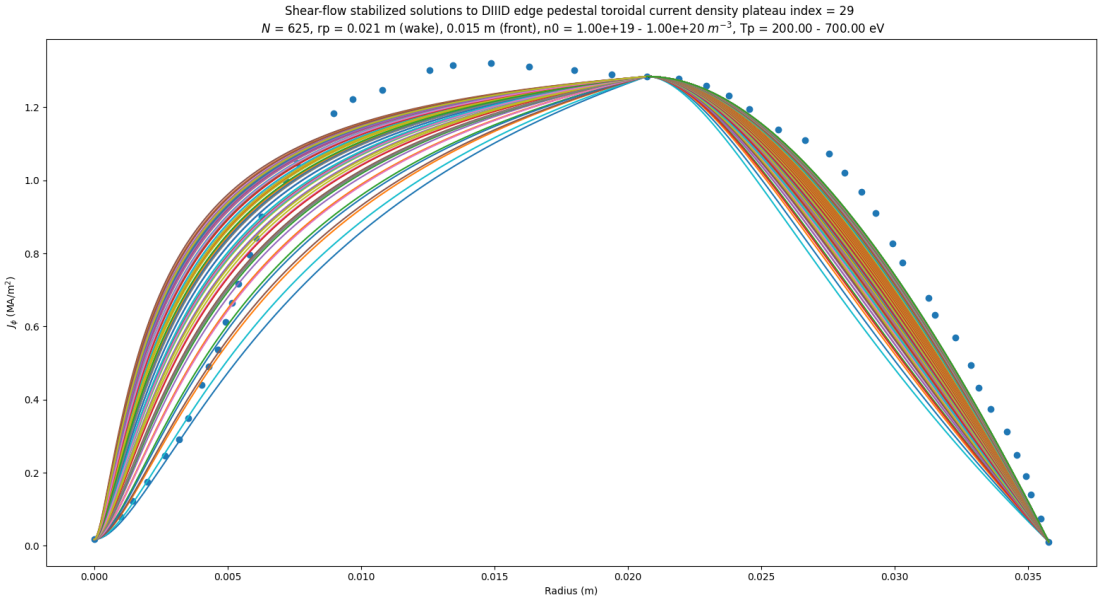


FIG. 8. Parameter sweep of the DIII-D edge pedestal across the span $n_0 \in [10^{19}, 10^{20}]$ m^{-3}, $T_p \in [200, 700]$ eV with $N = 25 * 25$ total value-pairs swept through. Every band represents a solution obtained from the analytic model here with less than 20% range-normalized relative root mean square error. The front region is to the right of the connection point, and the wake is to the left.

so we are left with two conditions for the axial and radial gradients,

$$\frac{\partial p}{\partial r} = 0 \tag{92}$$

$$\frac{\partial p}{\partial z} = \frac{\rho \nu}{r} \frac{\mathrm{d}}{\mathrm{d}r}\left(r \frac{\mathrm{d}u_z}{\mathrm{d}r}\right) \tag{93}$$

Equation (93) implies that,

$$p(r,z) = p_0(r) + 2u_{z,0}\rho\nu C z \left(\frac{2C - r}{(r+C)^4}\right) \tag{94}$$

and therefore from Equation (92) implies that,

$$\frac{\partial p}{\partial r} = \frac{\partial p_0}{\partial r} + 2u_{z,0}\rho\nu C z \left(\frac{3r - 9C}{(r+C)^5}\right) = 0 \tag{95}$$

From Equation (95) it is apparent that the radial pressure gauge must be uniform $p_0(r) = p_0$ because otherwise it would depend on z and the analysis would be inconsistent, or require external forces to be satisfied. Therefore, we can see that on $z = 0$, and $r = 3C$ the profile,

$$u_z(r) = u_{z,0} \frac{r^2}{(r+C)^2} \tag{96}$$

satisfies the 1D Navier-Stokes with a force free component, meaning no external forces are required when the pressure gauge is uniform. This is especially noteworthy because it means that along these loci this flavor of the equilibrium is valid regardless of the external forces.

RELATIVISTIC BENNETT EXCHANGE

The profile used in this paper has been based on a non-relativistic form of the approximate, self-similar, relativistic solution that Bennett obtained for the relativistic mass density which is,

$$\rho_1 = \rho_2 = \frac{\rho_0}{(1 + b\rho_0 r^2)^2} \tag{97}$$

$$b = \frac{\pi e^2}{2k_B c^2} \frac{(u+v)^2}{T_e + T_i} \tag{98}$$

In the relativistic case for a pure axial flow we have,

$$\rho_0 = mn = \gamma^2 m_0 n_0 \tag{99}$$

where m_0, n_0 are the rest mass and number density. For a singly-ionized hydrogen-electron plasma we then have,

$$u_z(r) = u_{z,0}\gamma(r) \frac{1}{(1 + b\gamma(r)^2 m_0 n_0 r^2)^2} \tag{100}$$

$$= u_{z,0} \frac{1}{\gamma^3} \frac{T^2(r)}{(T^2(r)\gamma^{-2} + C_B^{(R)} m_0 n_0 r^2)^2} \tag{101}$$

when the same exchange process is undertaken as previously. The γ dependence introduces formidable implicit structure into the axial flow, and this problem will be left for future work.

DISCUSSION

The shear-flow stabilized properties of the equilibrium derived here and the broad applicability it has shown to disparate regimes across fusion energy and plasma science demands further investigation. At the heart of this investigation are questions about where else this equilibrium might play a role, and what role higher-order energy and heat flux closures play.

Two of the main characteristic signatures of the equilibrium are an enhanced thermodynamic gradient, and a uniform density. In practice, the density of real plasmas is typically only approximately uniform, and the temperature gradient is typically not completely faithful to the idea of a cubic one which starts from absolute zero. However, despite these concerns, the accuracy observed here is still legitimate. It is not artificially produced, and indeed is derived from experimental values.

Two other characteristic signatures are a magnetic null on the axis, along with large shear layers in both the plasma current density and magnetic field. Because the plasma number density is treated as uniform, the axial current shear layer is associated with an underlying axial flow shear. The magnetic shear layer appears close to the edge of the pinch.

One topic which has not been touched on is the idea of a co-moving vortex, e.g.,

$$u_{z,e}(r) = u_{z,0e}\frac{r^2}{(r+C_e)^2} \tag{102}$$

$$u_{z,i}(r) = u_{z,0i}\frac{r^2}{(r+C_i)^2} \tag{103}$$

so that the center-of-mass flow is,

$$\vec{u} = u_{z,0i}\frac{m_i r^2}{(m_i+m_e)(r+C_i)^2} + u_{z,0e}\frac{m_e r^2}{(m_i+m_e)(r+C_e)^2}\hat{z}$$

with the drift supporting flow being,

$$\vec{U} = \vec{u}_i - \vec{u}_e = r^2\left(\frac{u_{z,0i}}{(r+C_i)^2} - \frac{u_{z,0e}}{(r+C_e)^2}\right)\hat{z} \tag{104}$$

if

$$\frac{u_{z,0i}}{u_{z,0e}} = \frac{(r+C_i)^2}{(r+C_e)^2} \tag{105}$$

then the current density drops to zero while the center of mass flow becomes,

$$\vec{u} = u_{z,0i}\frac{r^2}{(r+C_i)^2}\hat{z} \tag{106}$$

$$= u_{z,0e}\frac{r^2}{(r+C_e)^2}\hat{z} \tag{107}$$

so the magnetic field gradients become linked to the displacement currents in the system, and they become unsteady so that the electric field acquires a non-trivial curl as well.

A potentially important consequence concerns fusion burn. If a fusion plasma contains a substantial shear-flow stabilized component of the equilibrium considered here, then in general the fusion power density cannot be inferred from using the ideal gas law alongside an evaluation of the fusion reactivity. Shear-flow stabilized Z-pinches require non-ideal energy and heat flux closures for which the pressure, temperature, and internal energy need not retain the relationship implied by the ideal gas law. Therefore, fusion power must ultimately be evaluated from the underlying species distribution functions, or from higher-order thermodynamic closures which are sufficient to determine them. This distinction could become significant wherever strong localized shear and enhanced thermodynamic gradients coexist.

An enduring question that must be answered is where else does this equilibrium apply beyond the situations argued here? In astrophysical contexts extremely long length scales cause the Shumlak-Hartman criterion to relax when sufficient plasma number density is present, and this can lead the matter to organize according to Ideal MHD behavior if the Reynolds magnetic number grows large enough.

The geometrical requirements of the equilibrium also suggest several systems in which it may be worthwhile to search for this component directly. Helion's adiabatic FRC approach involves axially accelerated, current-carrying plasmoids merging together to undergo strong magnetic compression. This provides several of the ingredients that permit a localized shear-flow stabilized Z-pinch component, and data from a 2023 paper on the technology show an enhanced thermodynamic gradient in both the electrons and ions which coincides with a region of approximately uniform density[12].

The axisymmetric electrode, and discharge geometry publicly described for the Quantum Kinetics Corporation electro-physical transmutation device[13] likewise provide the ingredients necessary for this kind of component. For the small current densities observed a co-moving regime might be applicable which suggests an unsteady component that would give rise to large inertial forces on the lighter species due to the heavy ions are present, and any associated transient density modulations. This transient may therefore provide a mechanism worth investigating in connection with the reported signatures of beta decay and fusion-equivalent electron energies in this device. These observations do not establish the presence of the equilibrium. Spatially resolved measurements of flow, current density, plasma number density, temperature, and magnetic field would be required to test these hypotheses.

CONCLUSION

A shear-flow stabilized Z-pinch equilibrium has been derived from the non-relativistic Bennett profile. The profile requires an enhanced thermodynamic gradient, and leads to a tractable equilibrium that satisfies Ideal Magnetohydrodynamics because of its uniform density, and axisymmetric Z-pinch properties. It is also a 1D solution to Navier-Stokes with uniform viscosity.

The shear-flow stabilized properties are satisfied for

arbitrarily small plasma radius, and strongly satisfied for arbitrarily small pinch radius as the observation points move towards the axis.

Accurate solutions were obtained for three different plasma systems: the intensity of an air plasma streamer head, the axial flow velocity of shear-flow stabilized Z-pinches, and tokamak edge pedestals, using experimental data. Solving the boundary conditions requires solving for the roots of a quartic algebraic system. Some discrepancies exist between the calculated properties, and the experimental properties. For example, the experimental magnetic field of the Zap experiments is much larger than what is obtained from a single vortex. However, chains of vortices can be connected which closely match the sawtooth profiles reported, although the magnetic field still is not correctly obtained because of the uniform density approximation. Accurate values for thermal confinement time, peak shear, current density, and plasma pressure are obtained.

Beyond this, the flow roots are sometimes complex. The boundary conditions encode a depressed quartic system whose structure has not been investigated here, as this analysis is outside the scope of the present article whose primary purpose is to derive the equilibrium, and present the results obtained via the codes linked in the Data Availability Statement.

This is only a shear-flow stabilized zeroth-order component. Higher-order study of energy and heat flux closures is required in order to determine components beyond the first. The influence of anisotropic dissipative effects due to the large shear is also missing from this equilibrium. These are subjects for future study. An exhaustive effort should be performed to determine where this equilibrium can be found in fusion and industrial plasmas as this physics can give insight into the structure of plasma thermal lifetime. As a toy model, the equilibrium also requires further exploration theoretically.

ACKNOWLEDGMENTS

The author would like to acknowledge Aria Johansen for her feedback on the early manuscript; Ilya Dodin for his challenges made to the physicality of the equilibrium; Peter Thoreau, and James Penna for their support of the research; Jack Coughlin for discussions on non-ideal shear-flow stabilized behavior and dimensionless numbers; Iman Datta for discussions on MHD; Eric Meier for introducing the author to the topic of the Bennett Pinch; Whitney Thomas for encouragement towards theoretical physics; Nathan Williams for teaching the author how to get results in theoretical physics; Guy Ramon for giving the author his first opportunity to perform research in theoretical physics; Chris Weber for his condensed matter class, and teachings on graduate school; Richard Barber for his advice on graduate school; Phil Kesten for many discussions on theoretical physics with the author when they were an undergraduate; and Jim Antwood for his endorsement of the arXiv manuscript.

DATA AVAILABILITY STATEMENT

All datasets and codes used in the production of the results in this paper can be found in the open-source repository found here. The specific codes used in the production of this paper are listed, Zap 2001, Zap 2009 sawtooth, MAST 2023, DIII-D, Li et al. 2021, and the equilibrium profiles.

[1] U. Shumlak and C. W. Hartman, "Sheared flow stabilization of the $m = 1$ kink mode in Z pinches," Phys. Rev. Lett. **75**, 3285–3288 (1995).

[2] B. Kadomtsev, "Hydromagnetic stability of a plasma," Reviews of plasma physics **2**, 153–199 (1966).

[3] J. R. Angus, J. J. Van De Wetering, M. Dorf, and V. I. Geyko, "Eigenmode analysis of the sheared-flow z-pinch," Physics of Plasmas **27**, 122108 (2020).

[4] U. Shumlak, C. S. Adams, J. M. Blakely, B. J. Chan, R. P. Golingo, S. D. Knecht, B. A. Nelson, R. J. Oberto, M. R. Sybouts, and G. V. Vogman, "Equilibrium, flow shear and stability measurements in the Z-pinch," Nuclear Fusion **49**, 075039 (2009).

[5] W. H. Bennett, "Magnetically self-focussing streams," Physical Review, Volume 45 (1934).

[6] J. Allen and L. Simons, "The bennett pinch for non-relativistic electrons," J. Plasma Phys., vol. 84 (2018).

[7] U. Shumlak, R. P. Golingo, B. A. Nelson, and D. J. Den Hartog, "Evidence of stabilization in the Z-pinch," Phys. Rev. Lett. **87**, 205005 (2001).

[8] X. Li, S. Dijcks, S. Nijdam, A. Sun, U. Ebert, and J. Teunissen, "Comparing simulations and experiments of positive streamers in air: steps toward model validation," Plasma Sources Science and Technology **30**, 095002 (2021).

[9] R. J. Groebner and S. Saarelma, "Elements of h-mode pedestal structure," Plasma Physics and Controlled Fusion **65**, 073001 (2023).

[10] R. J. Jayakumar, S. L. Allen, K. H. Burrell, L. L. Lao, M. A. Makowski, C. C. Petty, and D. M. Thomas, "Current profile measurement on the DIII-D tokamak," Fusion Science and Technology **48**, 852–863 (2005), https://doi.org/10.13182/FST05-A1044.

[11] E. Rodríguez, P. Helander, and M. Landreman, "Generalized boozer coordinates: A natural coordinate system for quasisymmetry," Physics of Plasmas **28**, 092510 (2021).

[12] D. Kirtley and R. Milroy, "Fundamental scaling of adiabatic compression of field reversed configuration thermonuclear fusion plasmas," Journal of Fusion Energy **42**, 30 (2023).

[13] M. B. Lee, N. D. Ward, M. Leach, and R. Kent, "A resonant electrophysical transmutation method for water purification," Technical Report PNNL-SA-172771 (Pacific Northwest National Lab. (PNNL), Richland, WA (United States), 2022).